NASA TECHNICAL NOTE

NASA TN D-5500

c. 1

NASA TN D-5500

TECH LIBRARY KAFB, NM

0058416

LOAN COPY: RETURN TO
AFWL (WLOL-2)
KIRTLAND AFB, N MEX

FREE-STREAM ELECTRON CONCENTRATION IN AN ARC-HEATED WIND TUNNEL AND CORRELATION OF LANGMUIR PROBE AND MICROWAVE INTERFEROMETER MEASUREMENTS

by Roy J. Duckett and W. Linwood Jones, Jr.

Langley Research Center
Langley Station, Hampton, Va.

NATIONAL AERONAUTICS AND SPACE ADMINISTRATION • WASHINGTON, D. C. • OCTOBER 1969

TECH LIBRARY KAFB, NM

0058416

1. Report No. NASA TN D-5500	2. Government Accession No.	3. Recipient's Catalog No.
4. Title and Subtitle FREE-STREAM ELECTRON CONCENTRATION IN AN ARC-HEATED WIND TUNNEL AND CORRELATION OF LANGMUIR PROBE AND MICROWAVE INTERFEROMETER MEASUREMENTS		5. Report Date October 1969
		6. Performing Organization Code
7. Author(s) Roy J. Duckett and W. Linwood Jones, Jr.		8. Performing Organization Report No. L-6679
9. Performing Organization Name and Address NASA Langley Research Center Hampton, Va. 23365		10. Work Unit No. 129-01-22-01-23
		11. Contract or Grant No.
12. Sponsoring Agency Name and Address National Aeronautics and Space Administration Washington, D.C. 20546		13. Type of Report and Period Covered Technical Note
		14. Sponsoring Agency Code

15. Supplementary Notes

16. Abstract

Langmuir probes and microwave interferometer studies were made in the free stream of a Mach 10 arc-heated wind tunnel using air and nitrogen as test media. Electron concentrations were measured from 1×10^9 to 6×10^{10} electrons per cubic centimeter. The measured electron concentrations were compared with the finite-rate nonequilibrium calculations and were found to be about 1 order of magnitude greater for the case of air and several orders of magnitude for nitrogen. Several mechanisms are examined for the increased electron concentration. Correlation of the microwave interferometer and conical Langmuir probe measurements yielded results which agreed within a factor of 2. The mean electron temperature measured by the Langmuir probe was equal to the gas temperature at the throat of the nozzle.

17. Key Words Suggested by Author(s) Microwave Interferometers Langmuir probes Free-stream electron concentration of an arc-heated tunnel	18. Distribution Statement Unclassified – Unlimited

19. Security Classif. (of this report)	20. Security Classif. (of this page)	21. No. of Pages	22. Price*
Unclassified	Unclassified	38	$3.00

*For sale by the Clearinghouse for Federal Scientific and Technical Information
Springfield, Virginia 22151

FREE-STREAM ELECTRON CONCENTRATION IN AN ARC-HEATED WIND TUNNEL AND CORRELATION OF LANGMUIR PROBE AND MICROWAVE INTERFEROMETER MEASUREMENTS

By Roy J. Duckett and W. Linwood Jones, Jr.
Langley Research Center

SUMMARY

Langmuir probes and microwave interferometer studies were made in the free stream of a Mach 10 arc-heated wind tunnel using air and nitrogen as test media. Electron concentrations were measured from 1×10^9 to 6×10^{10} electrons per cubic centimeter. The measured electron concentrations were compared with the finite-rate nonequilibrium calculations and were found to be about 1 order of magnitude greater for the case of air and several orders of magnitude for nitrogen. Several mechanisms are examined for the increased electron concentration. Correlation of the microwave interferometer and conical Langmuir probe measurements yielded results which agreed within a factor of 2. The mean electron temperature measured by the Langmuir probe was equal to the gas temperature at the throat of the nozzle.

INTRODUCTION

Plasma generation and its relation to chemical kinetic phenomena in the free stream of low-density high-power, electric-arc-heated wind tunnels is not well understood. Frequently, the presence of ionization is desirable, as in the case of plasma power generators and accelerators; but whether the plasma formation is accidental or deliberate, a knowledge of the degree of ionization of the test gas is needed in order to define the composition of the gas for test purposes.

The use of free molecular electrostatic or "Langmuir" probes for diagnosing nonflowing plasmas has been well documented. (See refs. 1 and 2.) Several investigators have modified free molecular theory to consider the effect of a directed ion flow in a supersonic flowing plasma (ref. 3). The probes used in this investigation were of two types. The first consisted of a 0.075-millimeter-diameter iridium cylindrical probe 10 millimeters long. This probe was alined parallel to the flow and could be laterally surveyed from the tunnel wall to the center line. The second probe consisted of a 5° half-angle circular copper cone 50 millimeters long and mounted on the tunnel center line.

The results of an experimental investigation of the electron concentration and electron temperature in the test section of an arc-heated wind tunnel are presented and compared with the theoretical values. This report also gives the correlation between electron concentrations as determined from a microwave interferometer and the conical Langmuir probe. (In addition to determining the electron concentration and electron temperature in the free stream, the conical Langmuir probe was tested for future investigations.)

SYMBOLS

A	Avogadro number
a	surface area
℄	center line
d	thickness
E	electric field intensity
e	electronic charge
f	frequency
H	magnetic field intensity
h	Planck's constant
I	current
J	current density
K	Boltzmann's constant
k	constant
L	length
m	mass

$\overline{M}$	mean molecular weight
N	number density
n(x)	plasma distribution function
p	pressure
T	temperature
V	voltage
V^-	ionization potential
v	velocity
X	mole fraction
x	rectangular coordinate
α	fraction ionized
β	phase constant
γ	specific ion concentration
ϵ	permittivity
η	ratio of potential to kinetic energy
θ	phase, degrees
λ	wavelength
λ_D	Debye length
ν	frequency
ρ	density

$\Delta\phi$	phase shift in radians
ω	angular frequency, $2\pi f$
Ω	resistance, ohms

Subscripts:

A,B	detectors A and B
cr	critical
℄	center line
e	electron
i	positive ion
net	ions plus electron
o	vacuum
p	plasma
s	sheath
th	throat
t	arc heater stagnation conditions
∞	free stream
2	behind oblique shock
+	positive conventional current
-	negative

THEORY

Langmuir Probe

The free molecular theory for Langmuir probes in Maxwellian velocity distributed plasmas (ref. 4) requires that a probe collect electrons when it is biased positively with respect to the floating potential of the plasma. The saturated electron current density is related to the electron density by

$$J_- = \frac{N_e e v_e}{4}$$

where $v_e = \sqrt{\frac{8KT_e}{\pi m_e}}$ and is the electron random velocity.

When the probe is biased negatively, positive ions are collected and the saturation ion current density is related to the ion density by

$$J_+ = 0.4 N_i e v_i \tag{1}$$

where $v_i = \sqrt{\frac{2KT_e}{m_i}}$ and is the velocity with which ions reach the sheath.

As the voltage V applied to the probe varies between these extremes, the net current density is

$$J_{net} = J_- \exp\left(\frac{-eV}{KT_e}\right) - J_+ \tag{2}$$

Rearranging equation (2) and taking logarithms of both sides yields

$$\log\left(J_+ + J_{net}\right) = \log J_- - \left(\frac{eV}{KT_e}\right) \tag{3}$$

Therefore, if $\left(J_+ + J_{net}\right)$ is measured and plotted on semilog paper against V, the plot will be a straight line with a slope of e/KT_e. The electron temperature is then determined from this slope. (See fig. 1.)

Since in making probe measurements, one measures current rather than current density, two major conditions must be satisfied in order to interpret the probe voltage-current characteristics properly. First the plasma species mean free paths must be greater than the probe diameter to insure that the probe does not disturb the plasma. Next the dimensions of the plasma sheath form around the probe must be less than a mean free path to prevent collisions inside the sheath. Reference 4 describes a technique to reduce the requirement for a priori information in supersonic flowing plasmas by using a narrow wedge-shaped probe alined parallel to the flow.

The conical probe used in this investigation was similar in behavior to the wedge probe and had the advantage of high-current-collection capability and also a low-sheath-thickness correction factor. The sheath thickness d_s can be approximated by

$$d_s = \lambda_D \eta^{3/4} \tag{4}$$

where

$$\lambda_D = \sqrt{\frac{\epsilon_o K T_e}{N_e e^2}} = 7\sqrt{\frac{T_e}{N_e}} \text{ cm} \tag{5}$$

and

$$\eta = \left| \frac{eV}{KT_e} \right| \tag{6}$$

If typical values of 3×10^{10} electrons/cm^3 as a mean for the electron concentration with an electron temperature of 2500° K and an applied voltage of 5 volts are chosen, the sheath thickness is only 2.6×10^{-2} cm. This dimension was small compared with the mean diameter of the probe.

The saturation ion current I_+ collected by the probe will be

$$I_+ = 0.4 N_{i,\infty} e v_i a \tag{7}$$

When the probe is alined parallel to the supersonic plasma flow, the conical shock which is formed will be weak, since the cone angle is small. The flow will be turned through the cone half-angle, and at the surface it will be parallel to the surface of the probe. The plasma flow may be considered to be frozen when the time interval required for the flow to traverse the cone is less than the recombination time of the ions. The effect of the shock is to compress the gas and therefore the electron density by a known factor.

The current of the probe will then be

$$I_+ = 0.4 N_{i,\infty} e v_i \frac{\rho_2}{\rho_\infty} a \tag{8}$$

where ρ_2/ρ_∞ is the density ratio across the conical shock. All electron density calculations contained in this report were performed by using equation (8). An experimental study of the flow over this type of cone has been done by Hickman. (See ref. 5.)

The conical probe used in this investigation had a low temperature with large surface area for the collection of ions and slight perturbation of the stream flow. The disadvantage is that it does not have the high spatial resolution of small wire probes.

Microwave Interferometer

Analysis of the interaction of electromagnetic waves with a plasma shows that the phase of a transmitted wave can be related to the plasma electron density. Although the test facility is cylindrical, the proximity of the narrow beam microwave antennas makes it possible to consider the problem in one dimension, that is, a plasma slab. The plasma slab analogy is discussed in detail in reference 6.

The phase constants for vacuum and the low collision plasma are, respectively:

$$\beta_o = \frac{2\pi}{\lambda}$$

$$\beta_p = \left(1 - \frac{\omega_p}{\omega}\right)^{1/2} \frac{2\pi}{\lambda} = \left(1 - \frac{N_e}{N_{e,cr}}\right)^{1/2} \frac{2\pi}{\lambda} \tag{9}$$

where ω_p is $2\pi\left(8970\sqrt{N_e}\right)$ radians/cm^3 and $N_{e,cr}$ is $\dfrac{\omega^2}{3.17 \times 10^9}$ electrons/cm^3.

The phase change introduced by the plasma is then

$$\Delta\phi = \int \left(\beta_o - \beta_p\right) dx = \int \left\{1 - \left[1 - \frac{n(x)}{N_{e,cr}}\right]^{1/2}\right\} \frac{2\pi}{\lambda}\, dx \tag{10}$$

where the integration is carried out along the direct path between the transmitting and receiving horns. The preceding equation then becomes

$$\Delta\phi \approx \frac{\pi}{\lambda N_{e,cr}} \int n(x)\, dx = \frac{e^2}{2\epsilon_o N_{e,cr}\omega} \int n(x)\, dx \qquad \left(N_e \ll N_{e,cr}\right) \tag{11}$$

Therefore, for $N_e \ll N_{e,cr}$, the phase shift is an integral function of the electron concentration.

If the plasma slab is assumed to be homogeneous, for a given path L the average electron concentration becomes:

$$\overline{N}_e \int_0^L \frac{n(x)\, dx}{L} = \frac{2\epsilon_o N_{e,cr}}{e^2} \frac{\omega\, \Delta\phi}{L} = \frac{118.4}{2\pi L}\, \omega\, \Delta\phi \text{ cm}^{-3} \tag{12}$$

where ω is the angular frequency in radians/second, $\Delta\phi$ is the phase shift in radians, and L is the plasma thickness in centimeters.

In order to determine the value of L to use in the preceding equation, a fixed-bias cylindrical Langmuir probe survey was made at the test section. The results of the probe survey are shown in figure 2 and are discussed in a later section. Several Langmuir probe surveys provided an equivalent L of 28.0 cm. The value of L was determined by integrating the area under the curve in figure 2 and calculating an equivalent homogeneous slab thickness. Substituting the frequency of the microwave signal

$f = 24 \times 10^9$ hertz and converting $\Delta\phi$ from radians to degrees yields

$$\bar{\bar{N}} = 1.772 \times 10^9 \, \Delta\theta \ \text{cm}^{-3} \tag{13}$$

where $\Delta\theta$ is the phase shift in degrees. This equation was then used to calculate the electron concentration in the test section.

EXPERIMENTAL APPARATUS

Langmuir Probe

The Langmuir probe used in this investigation was a 5° half-angle cone and is shown in figure 3. The probe consisted of three main parts, a conical copper ion collector, a truncated conical boron nitride insulating section, and a copper sting support which also served as the electron collector. As discussed in the section on probe theory, the ion collector length and base diameter were made very much greater than 2.6×10^{-2} cm, the positive ion sheath thickness, to minimize sheath effects.

The ion collector was cooled by a closed cycle system using deionized water which maintained a high electrical resistance to the electron collector. The probe circuit diagram is shown in figure 4. The ion collector was biased negatively with respect to the tunnel walls by a -1.5-volt battery. A 10- to 100-hertz triangular sweep signal was applied in series to the probe by means of an isolation transformer. The voltage of the triangular wave was set at approximately ±3.5 volts peak so that the probe potential went from +2 volts to -5 volts with respect to the tunnel walls. The voltage and current wave forms were recorded on a high-speed oscillograph. There was one channel for probe bias and two channels for probe current. Figure 5 shows typical data for one cycle of the swept bias voltage.

In addition to the conical probe, a movable cylindrical probe with its axis alined parallel to the flow was used for temperature surveys and for determining the density profile across the tunnel. This probe had a diameter of 0.075 mm and was used with fixed and swept voltage. The circuit for these measurements was the same as that of figure 4.

Microwave Interferometer

A 24-GHz microwave interferometer was used to provide an independent, nonperturbing measurement of the electron density in the arc tunnel. The interferometer is basically a bridge circuit which compares the phase of the signal in the data path with that of the signal in the reference path. When a plasma is inserted between the horn antennas, the data path signal undergoes a negative phase shift relative to the undisturbed phase of the reference path. As discussed previously, the measured phase shift in the data path can be related to the integrated value of the electron density distribution of the plasma. A diagram of the experimental setup is shown in figure 6 and a detailed discussion of system operation is given in the appendix.

The microwave energy was transmitted across the tunnel diameter by horn antennas mounted in opposite access ports. The Langmuir probe was located approximately 3 inches downstream of the microwave station. No appreciable gradients are expected over this 3-inch distance.

Serious problems can occur in the test section because of multipath propagation, which is caused by the microwave energy being reflected off the Langmuir probe or tunnel walls and interfering with the energy which propagates directly between the antennas. To minimize this effect, the rectangular access ports were lined with microwave absorption material.

Two tests were conducted to check for multipath effects. The first was to monitor the phase and amplitude of the received microwave signal while a 6-inch-square (15.24 cm) metal plate is moved horizontally along the tunnel walls parallel to but not intersecting the microwave beam and also the plate is moved vertically perpendicular to the axis of the beam in the vicinity of the Langmuir probe station. Changing the position of the metal plate, which is highly reflective to microwaves, would cause definite phase variations of the received signal if multipath effects were a problem. The absence of measurable variations in the received microwave signal during this test verified that multipath propagation could be neglected. Secondly, phase-shift measurements were performed by placing dielectric foam slabs between the microwave horn antennas. The foam slabs had relative dielectric constants of 1.02 to 1.5 and all were 6 inches square (15.24 cm) by 1 inch (2.54 cm) thick. Phase shifts were not affected by the distance from the sample to either antenna. The measured values agreed with theoretical calculations within ±10 percent.

Description of Facility

A diagram of the Langley 1-foot (0.305 m) hypersonic arc tunnel is shown in figure 7, and a description of the tunnel can be found in references 7 and 8. An analysis of the accuracy of test conditions is given in reference 9.

This facility uses a 1-megawatt dc power supply and operates at stagnation pressures of 10 to 25 atmospheres with stagnation enthalpies of 1500 Btu/lb to 4000 Btu/lb $\left(3.5 \times 10^{6}\text{ joules/kg to } 9.3 \times 10^{6}\text{ joules/kg}\right)$ with free-stream Mach numbers of 10 to 13. All the measurements were made at approximately 10 atmospheres and at a Mach number of 10. The range of temperatures was obtained by varying the mass flow and/or power to the arc heater.

RESULTS AND DISCUSSION

Predicted and Measured Electron Concentrations (Air)

Langmuir probe and microwave studies were made in the free stream of the Langley 1-foot (0.305 m) hypersonic arc tunnel. Electron concentrations were measured from 1×10^9 to 6×10^{10} electrons/cm^3. A computer program using 11 reactions and 1 ion species for air was used to predict the finite-rate nonequilibrium and frozen nonequilibrium electron concentration in the free stream. This program may be found in reference 10. This program was modified to include singularly ionized molecular nitrogen and oxygen ions but no significant differences were found. The measured microwave values for air (fig. 8) was one order of magnitude higher than those of the predicted values but approximately equal to the frozen flow value. Although the electron concentration agrees with the pure air frozen solution, possible contamination of copper particles from the arc heater electrodes was also considered as a source of electrons. The Saha equation was used to calculate the electron concentration at the throat of the arc heater for various levels of copper contamination.

The Saha equation is discussed in references 11 and 12 and may be expressed as follows:

$$\log\left(\frac{\alpha 2}{1 - \alpha}\, pX\right) = 2.5 \log T - 5041 \frac{\bar{V}}{T} - 6.491 \tag{14}$$

Since the stagnation pressure of the arc heater is 10 atmospheres, this resulting high density makes it reasonable to assume that thermodynamic equilibrium exists to the nozzle throat station. The fraction of ionized particles at the throat α may be calculated for a given mole fraction X from a knowledge of the ionization potential of copper, the throat temperature, and the pressure. The electron or ion concentration is then calculated from

$$\gamma = \frac{\alpha X}{\bar{M}} \tag{15}$$

If it is assumed that the flow is frozen at the throat, the electron concentration in the free stream becomes

$$N_e = \gamma \rho_\infty A \tag{16}$$

The results of these calculations may be seen in figure 8. The electron concentration could therefore be explained by contamination from copper and a frozen flow expansion. In this case the ion would be copper.

Mass Spectrograph Analyses of Stream Samples (Air)

In the previous discussion, it has been assumed that the air has been heated up to the stagnation temperature, but in the arc heater, part of the air is first heated to a higher temperature in passing through the arc. This air is then mixed with relatively cool air, which does not pass through the arc, and the mixture is cooled by the water-cooled walls of the stagnation chamber.

To determine whether the air in passing through the arc and then being cooled to stagnation temperature would have a different amount of nitrogen dissociated than predicted at normal stagnation conditions, an experiment was designed to measure the nitric oxide concentration in the free stream. The production of nitric oxide and the nitric oxide ion may be seen from the following chemical equations:

$$N_2 + N_2 \rightleftarrows 2N + N_2$$

$$N + O_2 \rightleftarrows NO + O$$

$$N + O \rightleftarrows NO^+ + e$$

$$O + N_2 \rightleftarrows NO + N$$

The nitric oxide concentration would indicate the degree of chemical nonequilibrium effects in the stagnation region of the arc heater. A drawing of the sampling apparatus is shown in figure 9. After the flow in the tunnel was well established, the valves between the probe and the vacuum were opened and the gas was allowed to flow through the sample bottle. After a sufficient time for the sample gas to replace the original gas, the vacuum valves were closed and the sample was analyzed with a mass spectrometer.

Although nitric oxide reacts rapidly with oxygen at atmospheric pressure to produce nitrogen dioxide ($2NO + O_2 \rightarrow 2NO_2$), when the sample was taken at reduced pressure (60 microns) the rate of reaction is believed to be sufficiently low to not affect the determination. This result was verified by performing successive spectrographic analyses and noting the rate of disappearance of the NO in the sample.

The results of the spectrographic analyses are shown in figure 10. As can be seen from these results, there is not an excessive amount of nitric oxide present.

One other possible source of available energy for electron production is radiant energy from the arc. A photon may ionize an atom or molecule if the photon has energy corresponding to the ionization energy of the atom or molecule. For ionization $h\nu$ of the photon must be greater than the ionization potential of the atom or molecule. Also, as the energy of the photon is increased beyond that required for ionization, the probability of ionization decreases. Therefore, photoionization is highly selective and depends upon the spectra of the radiation. Since the spectra of the high-pressure high-current arc are unknown particularly in the vacuum ultraviolet region where photoionization would occur, it can only be proposed as a possible production mechanism.

Predicted and Measured Electron Concentration (Nitrogen)

To avoid the complicated chemistry of air, the test gas was changed to nitrogen and the electron concentration was determined. Calculations of the electron concentration were based upon a chemical-kinetic model for nitrogen involving nine reactions and two ion species. The computer program in reference 9 was modified to accept the following equations:

$$N_2 + N_2 \rightleftarrows N_2 + 2N$$

$$N_2 + N \rightleftarrows N + 2N$$

$$e^- + N_2^+ \rightleftarrows 2N$$

$$e^- + N^+ + N \rightleftarrows N + N$$

$$e^- + N_2^+ + N \rightleftarrows N + N_2$$

$$e^- + N^+ + N_2 \rightleftarrows N_2 + N$$

$$e^- + N_2^+ + N_2 \rightleftarrows N_2 + N_2$$

$$e^- + N^+ + e^- \rightleftarrows e^- + N$$

$$e^- + N_2^+ + e^- \rightleftarrows e^- + N_2$$

The reaction rates and necessary constants may be found in reference 13. The results of the microwave experiments with nitrogen may be seen in figure 8. The finite-rate nonequilibrium calculations for nitrogen were less than 10^8 electrons/cm^3. Whereas, in the case of air the electron concentration could be explained by assuming that the expanded flow was frozen at throat conditions, the nitrogen results cannot be explained by this method. Possible Cu ionization in the flow, for the case of N_2, would be the same as that calculated for the Saha equation previously. (See fig. 8.) Quite obviously, this explanation is wrong since at the low temperatures it would require an unrealistic copper particle contamination of 30 percent, whereas at the higher temperatures a decrease of four orders of magnitude would be required. In the air experiments, the electron concentration could be explained by either a chemically frozen air expansion or because of contamination from copper particles with frozen expansion, but the nitrogen experiments cannot be explained by either case. Therefore, the production of electrons in nitrogen must be from some source other than those considered.

At a given pressure, increasing the gas temperature causes a more rapid approach to thermal equilibrium. However, if photoionization is occurring, this condition would represent a constant source of electrons and the overall level of electron concentration would be higher. Another possibility also exists and should be discussed. From the Langmuir probe and microwave measurements, fluctuations in the electron concentration by a factor of 2 were observed in the free stream. This condition is probably due to inadequate mixing of the plasma in the stagnation chamber of the arc heater. This relatively small effect could not explain the large discrepancy between theory and measurements.

The electron concentration as determined by the conical Langmuir probe using equation (8) and the copper ion can be seen in figure 11. If the ion was different in air and nitrogen, the calculated electron concentration in air and nitrogen would be different by a factor of $\sqrt{\frac{2KT_e}{m_i \pm \Delta m_i}}$ where Δm_i is the mass difference of the ions.

Figure 11 shows that no distinction can be made between the values for nitrogen and air. In any case there is agreement between the electron density as determined by the Langmuir probe and the microwave interferometer. This agreement may be fortuitous but in this case the conical Langmuir probe shows a linear relationship with the microwave value and therefore may be adjusted with an arbitrary constant to give the electron concentration.

Electron Temperature Measurements

As indicated in the section on theory, the determination of electron temperature depends upon the slope of the curve of log electron current plotted against probe voltage. (See fig. 1.) Determination of the slope may be subject to variation in reading by individuals and to the uncertainty of interpretation of a given measurement. The mean deviation was determined in order to ascertain the significance of the electron temperature measurements.

One measurement was checked by having several people reduce the data to determine the electron temperature independently. The repeatability of the interpretations was $\pm 200^{\circ}$ K from the mean value. Ten determinations of this measurement were made. Next, 16 different measurements were made of a single run. Values of this particular run varied from 4732° K to 3225° K. The mean value of these measurements was 3745° K with a mean deviation of 278° K. Since the mean deviation is greater than the reproducibility of a single measurement, the differences between the values are significant.

The relationship between the electron temperature of the free stream in the test section and the nozzle throat was determined. The throat temperature was predicted from the stagnation temperature by using the nonequilibrium program described in reference 10, and the ratios of electron temperature to throat temperature $\left(T_e/T_{th}\right)$ was determined. From a set of 50 measurements, this ratio had a mean value of 1.000 with a mean deviation of 0.243 and a standard deviation of 0.321.

Lateral surveys of electron temperature measurements were made with the cylindrical Langmuir probe in the test section for both nitrogen and air. The equipment used was the same as that in figure 4. The time required for one survey was approximately 1 second. The result of the survey may be seen in figures 12(a) and 12(b). The electron temperature in nitrogen remains constant from a location close to the wall to the tunnel center line. The electron temperature distribution in air, however, is lower at the walls of the test section and increased monotonically to the center line of the free stream.

The difference in results between nitrogen and air is another interesting feature. The electron concentration in nitrogen has been shown to be relatively constant for a wide variation in tunnel stagnation temperature as contrasted to the air data and the theoretical models postulated.

CONCLUSIONS

A microwave interferometric technique and Langmuir probe have been used to measure the electron concentration in the Mach 10 free stream of an electric-arc-heated hypersonic wind tunnel. The Langmuir probe technique also yielded electron temperature measurements. All measurements were made for a wide range of tunnel stagnation temperatures and for both air and nitrogen as test media. Significant conclusions are:

1. The microwave and the Langmuir probe measurements of electron concentration agree within a factor of 2.

2. The tests in air showed that the electron concentration was about an order of magnitude higher than the predicted finite-rate nonequilibrium value and was strongly dependent on the tunnel stagnation temperature. The electron concentration measurements made in nitrogen were several orders of magnitude higher than the predicted finite-rate values and were only weakly dependent on the tunnel stagnation temperature.

3. In air, if the gas flow is assumed to be frozen at the throat, the measured electron concentration is in agreement with calculated values. The measured electron concentration however could also be explained by ionization of copper, from the electrodes, in the stagnation region of the arc heater followed by a frozen-throat expansion.

4. The measured electron concentration in nitrogen cannot be explained by conclusion 3.

5. Langmuir probe measurements indicated that the mean electron temperature on the center line of the test section was the same as the temperature of the flow in the throat of the hypersonic nozzle for both air and nitrogen.

Langley Research Center,
National Aeronautics and Space Administration,
Langley Station, Hampton, Va., July 31, 1969.

APPENDIX

The 24-GHz Interferometer

The 24-GHz (K-band) interferometer was to provide a nonperturbing measurement of plasma electron densities of 7×10^{12} electrons/cm^3 or less. The microwave block diagram is shown in figure 13. The system is fabricated by using type WR-42 wave guides and is operated within the frequency range 24 GHz ± 0.5 GHz. A klystron oscillator, frequency stabilized by an oscillator synchronizer, delivers 100 milliwatts (mW) continuous wave output power. The interferometer utilizes a sine-cosine comparison technique (ref. 14), to measure the phase of the microwave signal. In this method, a continuous-wave carrier and a double sideband suppressed carrier (DSSC) signal are compared in a phase bridge.

The phase bridge is a microwave hybrid circuit and is shown in figure 14. The signal E_1 is the 24-GHz carrier supplied to port 1 by the reference phase path. The data signal E_2 is a DSSC signal with the sidebands located 1 KHz from the carrier frequency. A balanced modulator in the data path is used to produce the DSSC signal. The power level of the signal at port 1 is 10 mW and at port 2 is 0.01 mW or less. The waveguide path from port 1 to the detectors A and B is such that the signals arrive in phase and with equal amplitudes. The path from port 2 to the detectors A and B is such that the signals arrive with equal amplitudes but with a 90° difference in their phases. The phasor addition of E_1 and E_2 at the detectors is shown in figure 15. The resultant R of this addition is a 24-GHz carrier that is both amplitude- and phase-modulated at a 1-KHz rate. Since the crystal detector responds only to the magnitude of the electric field, the detector audio output is a 1-KHz sine wave. The amplitude of the 1-KHz signal is a function of the magnitude of the resultant which, in turn, is a function of the angle between the signal E_i and the suppressed carrier of E_2. It can be shown (ref. 15) that the output of detector A is $k_A \cos \theta$ and the output of detector B is $k_B \sin \theta$. The term k accounts for the amplitudes of the resultant and the diode characteristics. If the detectors are matched and if all the power divisions in the phase bridge are equal, then $k_A = k_B$. The ratio of the 1-KHz signal at detectors B and A is

$$\frac{k \sin \theta}{k \cos \theta} = \tan \theta$$

The ratio is therefore independent of amplitude changes in both signals and is only a function of the relative phase angle.

Figure 16 is a block diagram of the electronic portion of the interferometer. This system utilizes logarithmic signal processing to provide a continuous measurement of phase angles. This system is a significant improvement over previously reported systems which utilize ratio meters and provide continuous measurement over only one decade of $\tan\theta$. The 1-KHz signals from the microwave phase bridge are amplified in a tuned amplifier with a half power bandwidth of 200 Hz. The signals are then rectified by a bridge circuit and integrated in resistance-capacitance low-pass filter with an integration time of 0.01 second. The output of each integrator is logarithmically amplified and then subtracted in a differential amplifier. The output of the differential amplifier is recorded and represents the $\log\tan\theta$. Figure 17 illustrates the output of the differential amplifier with phase. Because of slight deviations in the logarithmic response of the amplifiers, the precision phase shifter, rather than mathematical law, is used to calibrate the recorder output. The phase shifter calibration accuracy is $\pm 2^\circ$ over the 360° range; however, for excursions of 5° or less, the accuracy is $\pm 0.2^\circ$. The maximum phase sensitivity occurs at 0° and 90° where the $\log\tan\theta$ goes from $-\infty$ to $+\infty$, respectively, (in practice the maximum obtainable $\tan\theta$ values were approximately 100). A phase ambiguity of 90° exist in the recorder output.

To reduce the ambiguity to 180°, a mechanical phase modulator was added in the data path. A motor-driven cam inserts a dielectric slab into the waveguide to shift the phase in a positive direction approximately 15°. Figure 18 shows the effect of the phase modulator on the recorder output. The direction of the pulses on the recorder output indicates an increasing positive phase shift and thereby reduces the phase ambiguity from 90° to 180°. For attenuation levels up to 20 dB in the data phase path, the phase recorder output changes less than $\pm 2^\circ$ throughout the entire 0° to 180° range.

REFERENCES

1. Lam, S. H.: Unified Theory for the Langmuir Probe in a Collisionless Plasma. Phys. Fluids, vol. 8, no. 1, Jan. 1965, pp. 73-87.

2. Laframboise, James G.: Theory of Spherical and Cylindrical Langmuir Probes in a Collisionless, Maxwellian Plasma at Rest. Rep. No. 100, Inst. Aerosp. Studies, Univ. Toronto, June 1966. (Available from DDC as AD 634596.)

3. Sonin, Ain A.: Free-Molecule Langmuir Probe and Its Use in Flowfield Studies. AIAA J., vol. 4, no. 9, Sept. 1966, pp. 1588-1596.

4. Scharfman, W. E.: The Use of Langmuir Probes To Determine the Electron Density Surrounding Re-Entry Vehicles. SRI Project 5034 (Contract NAS1-3942), Stanford Res. Inst., June 1965.

5. Hickman, Roy Scott: An Experimental Study of Hypersonic Rarefied Flow Over a 10° Cone. Rarefied Gas Dynamics, vol. 2, C. L. Brundin, ed., Academic Press, Inc., c.1967, pp. 1067-1085.

6. Heald, M. A.; and Wharton, C. B.: Plasma Diagnostics With Microwaves. John Wiley & Sons, Inc., c.1965.

7. Boatright, W. B.; Stewart, R. B.; and Sebacher, D. I.: Testing Experience and Calibration Experiments in a Mach Number 12, 1-Foot Hypersonic Arc Tunnel. Third Hypervelocity Techniques Symposium, Univ. of Denver and Arnold Eng. Develop. Center, Mar. 1964, pp. 182-212.

8. Boatright, W. B.; Sebacher, D. I.; Guy, R. W.; and Duckett, R. J.: Review of Testing Techniques and Flow Calibration Results for Hypersonic Arc Tunnels. AIAA Paper No. 68-379, Apr. 1968.

9. Duckett, Roy J.; and Sebacher, Daniel I.: Velocity Measurements in the Langley 1-Foot (0.305-Meter) Hypersonic Arc Tunnel. NASA TN D-3308, 1966.

10. Lordi, J. A.; Mates, R. E.; Moselle, J. R.: Computer Program for the Numerical Solution of Nonequilibrium Expansions of Reacting Gas Mixtures. Rep. No. AD-1689-A-6 (Contract No. NASr-109), Cornell Aeron. Lab., Inc., Oct. 1965.

11. Huber, Paul W.: Deduction of Reentry Plasma Properties About Manned Orbital Spacecraft From Radio Signal Attenuation Data. NASA TN D-4118, 1967.

12. Buchanan, Robert S.: Study of a Seeded Plasma. ARL 62-310, U.S. Air Force, Mar. 1962.

13. Dunn, M. G.; Daiber, J. W.; Lordi, J. A.; and Mates, R. E.: Estimates of Nonequilibrium Ionization Phenomena in the Inviscid Apollo Plasma Sheath. NASA CR-596, 1966.

14. Cohn, Seymour B.; and Oltman, H. George: A Precision Microwave Phase-Measurement System With Sweep Presentation. 1961 IRE International Convention Record, vol. 9, pt. 3, Inst. Radio Eng., Mar. 1961, pp. 147-150.

15. Panter, Philip F.: Modulation, Noise, and Spectral Analysis Applied to Information Transmission. McGraw-Hill Book Co., c.1965.

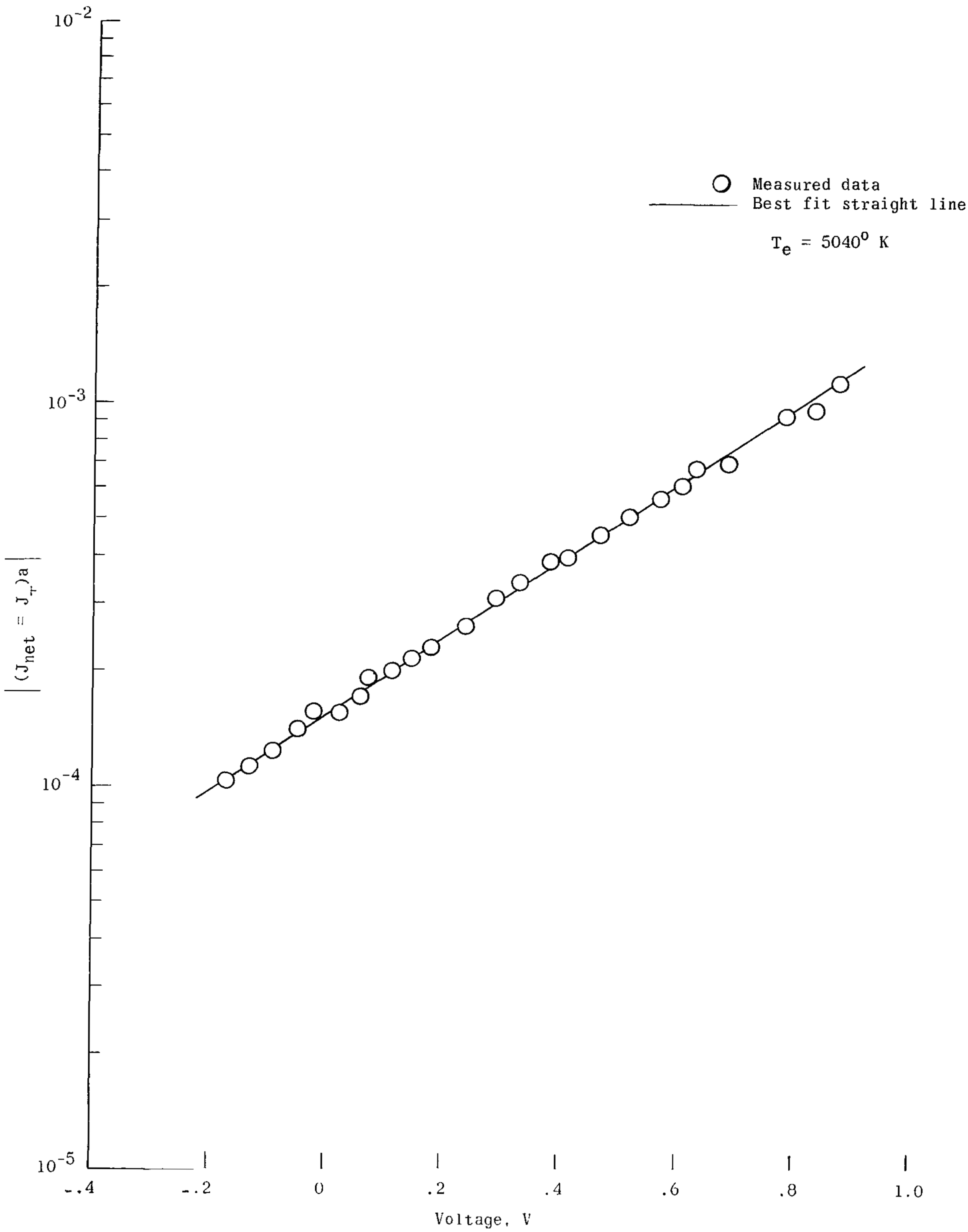

Figure 1.- Electron current as a function of applied voltage to the conical Langmuir probe.

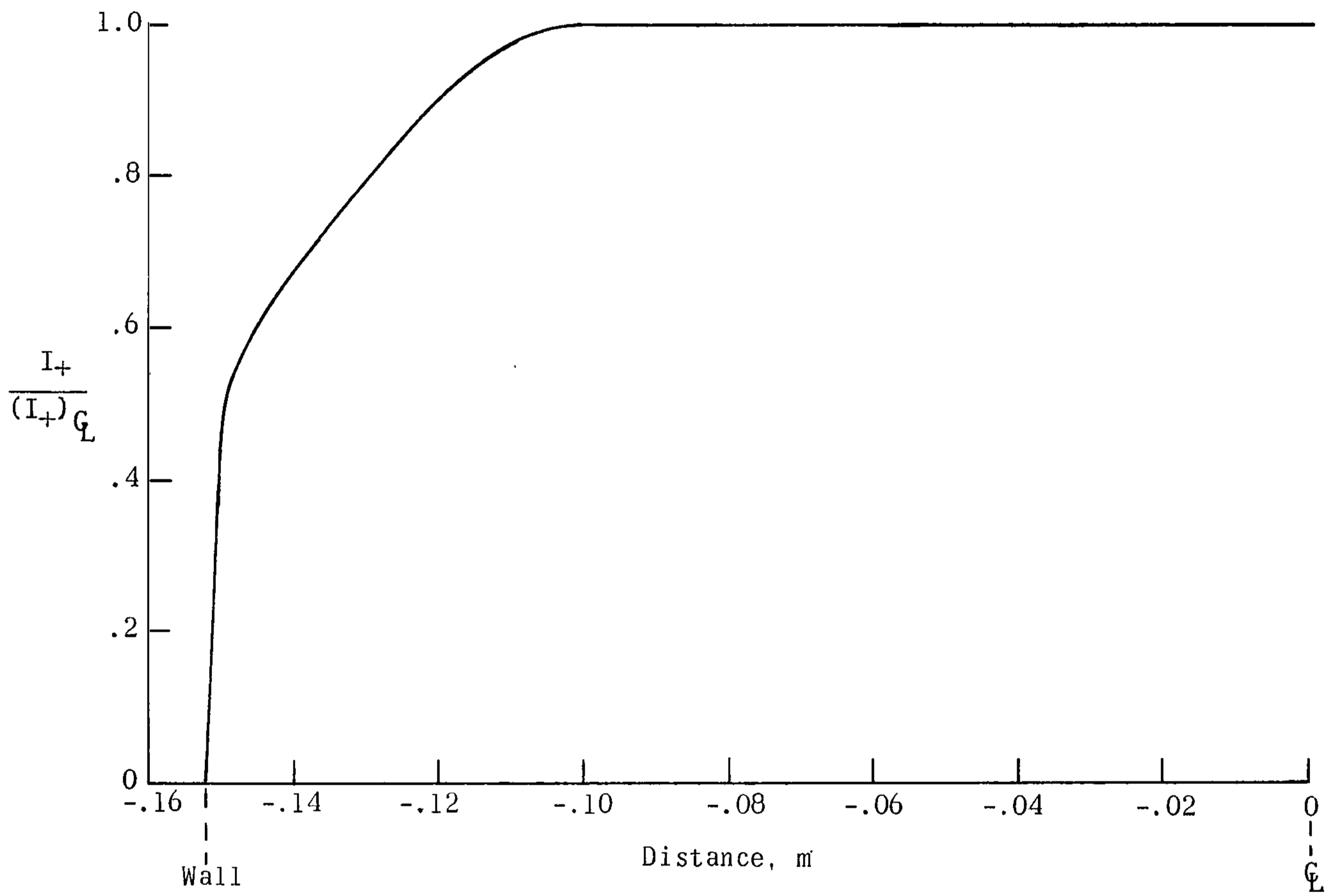

Figure 2.- Fixed-bias cylindrical Langmuir probe ion current survey of test section.

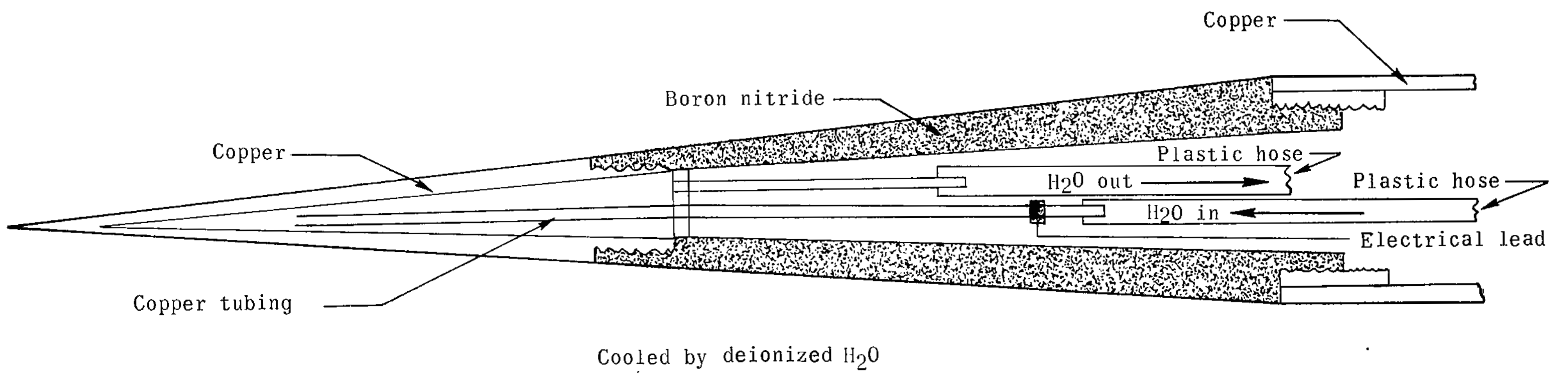

Figure 3.- Water-cooled Langmuir probe.

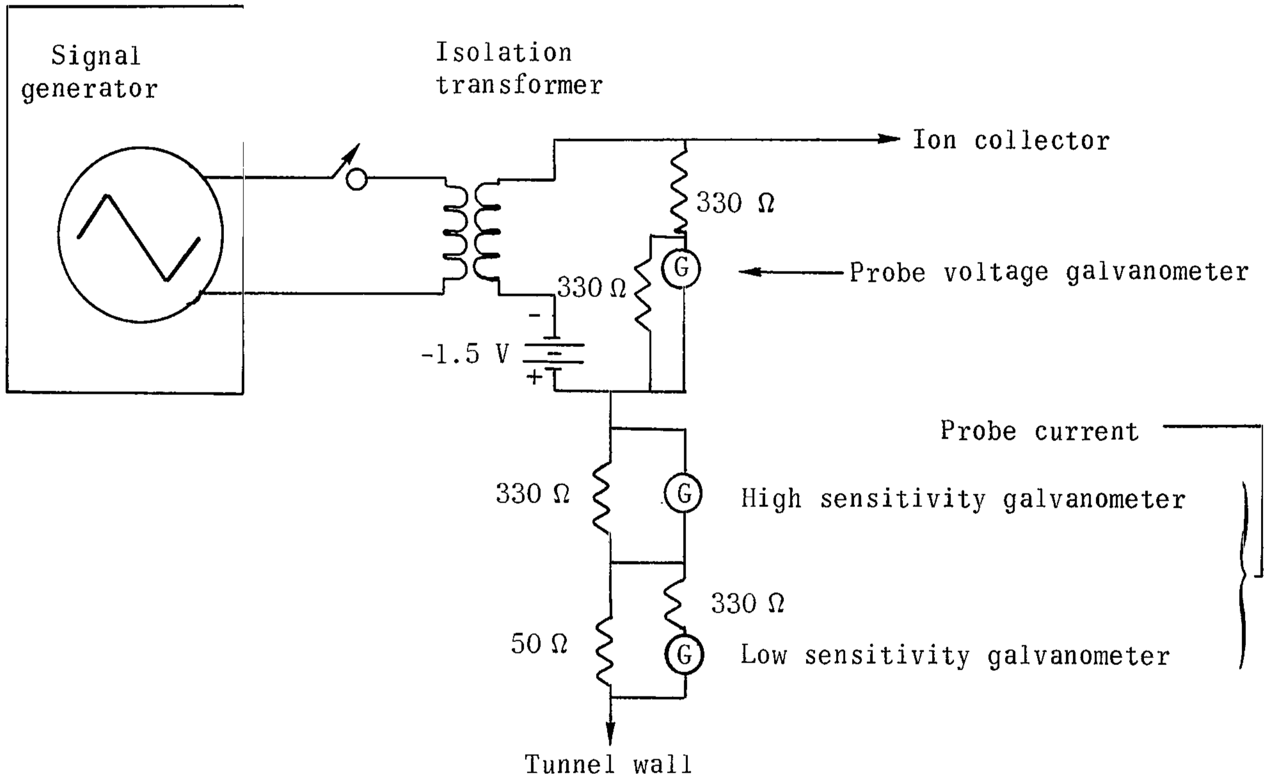

Figure 4. Langmuir probe circuitry.

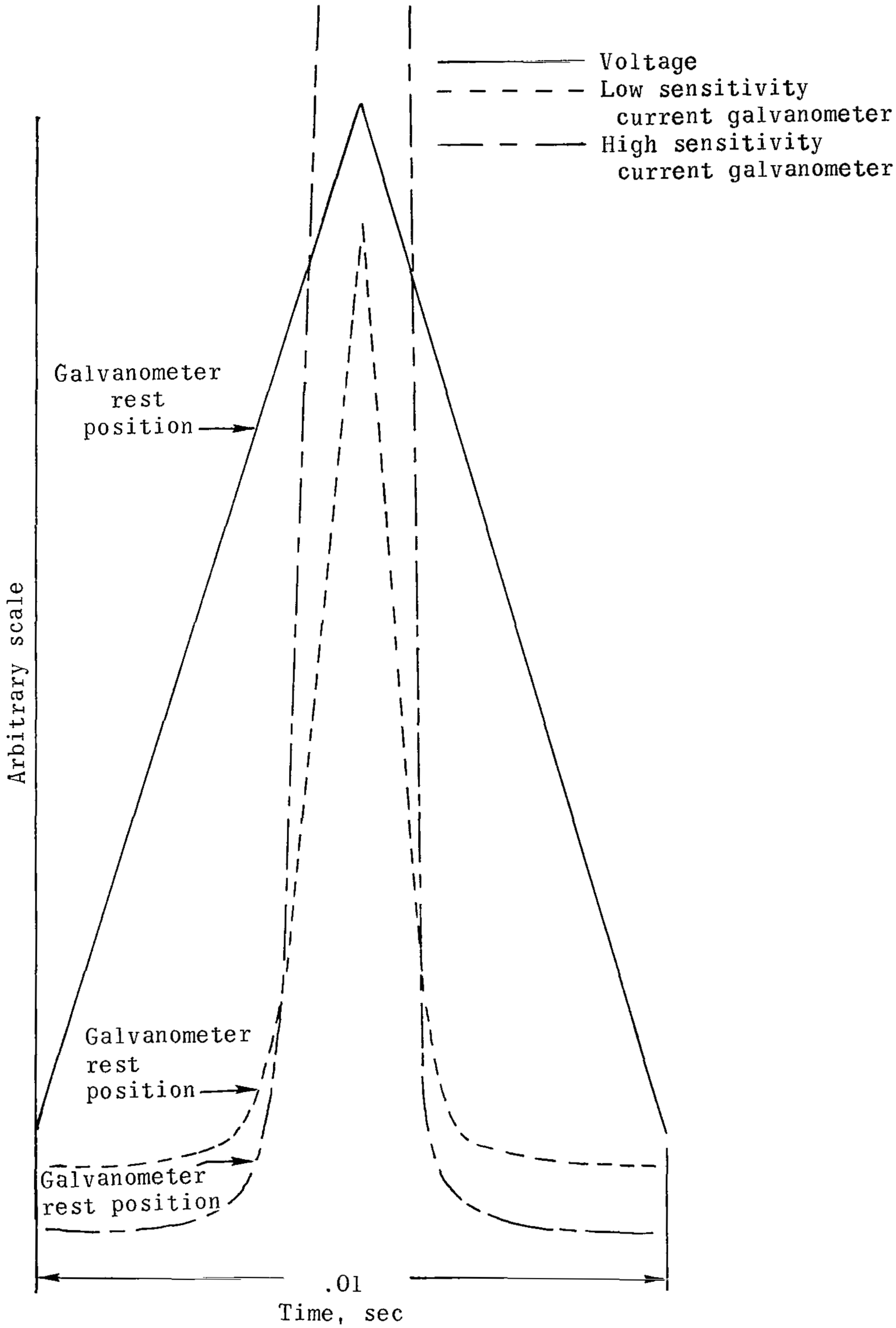

Figure 5.- Typical galvanometer deflection for swept Langmuir probe.

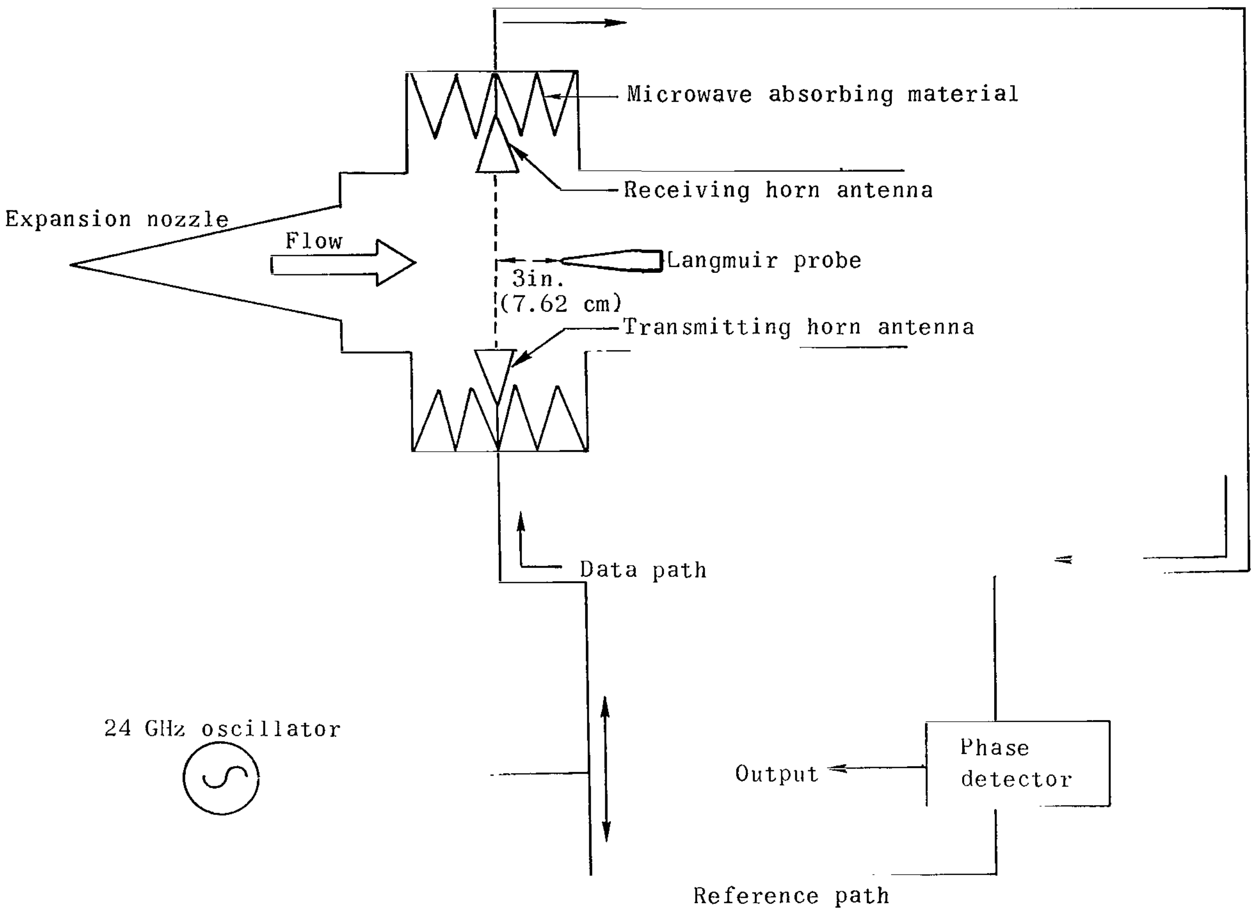

Figure 6.- Diagram of microwave interferometer apparatus in test section.

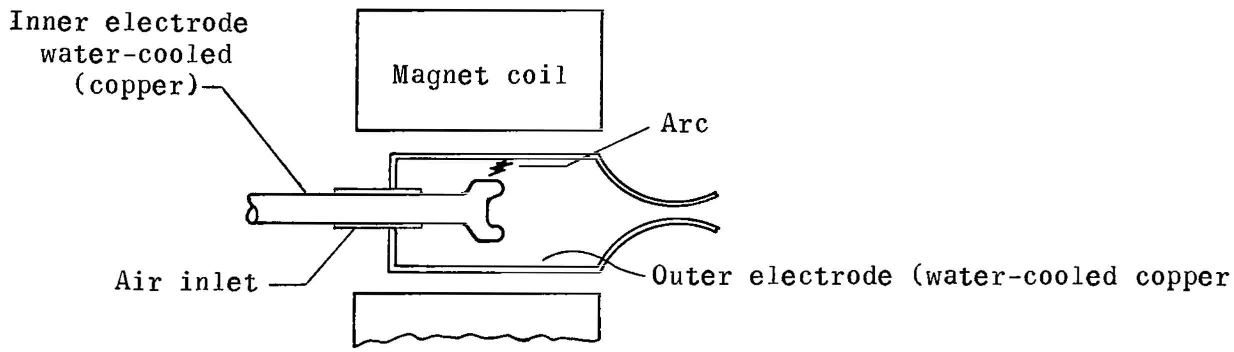

Arc heater configuration

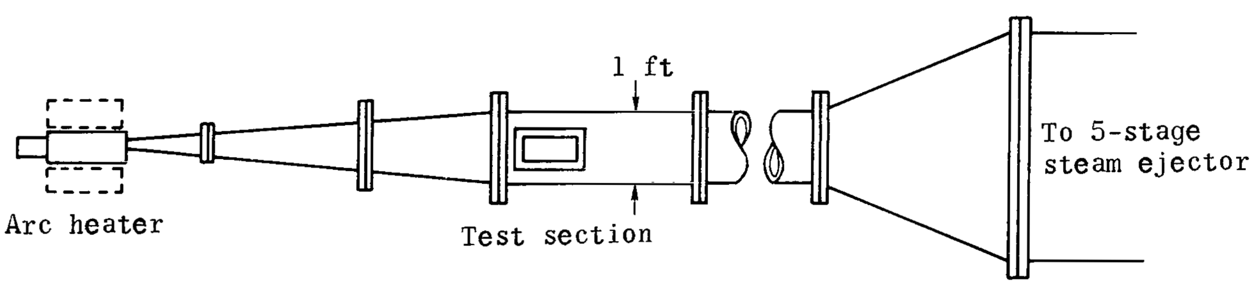

Figure 7.- Diagram of Langley 1-foot hypersonic arc tunnel.

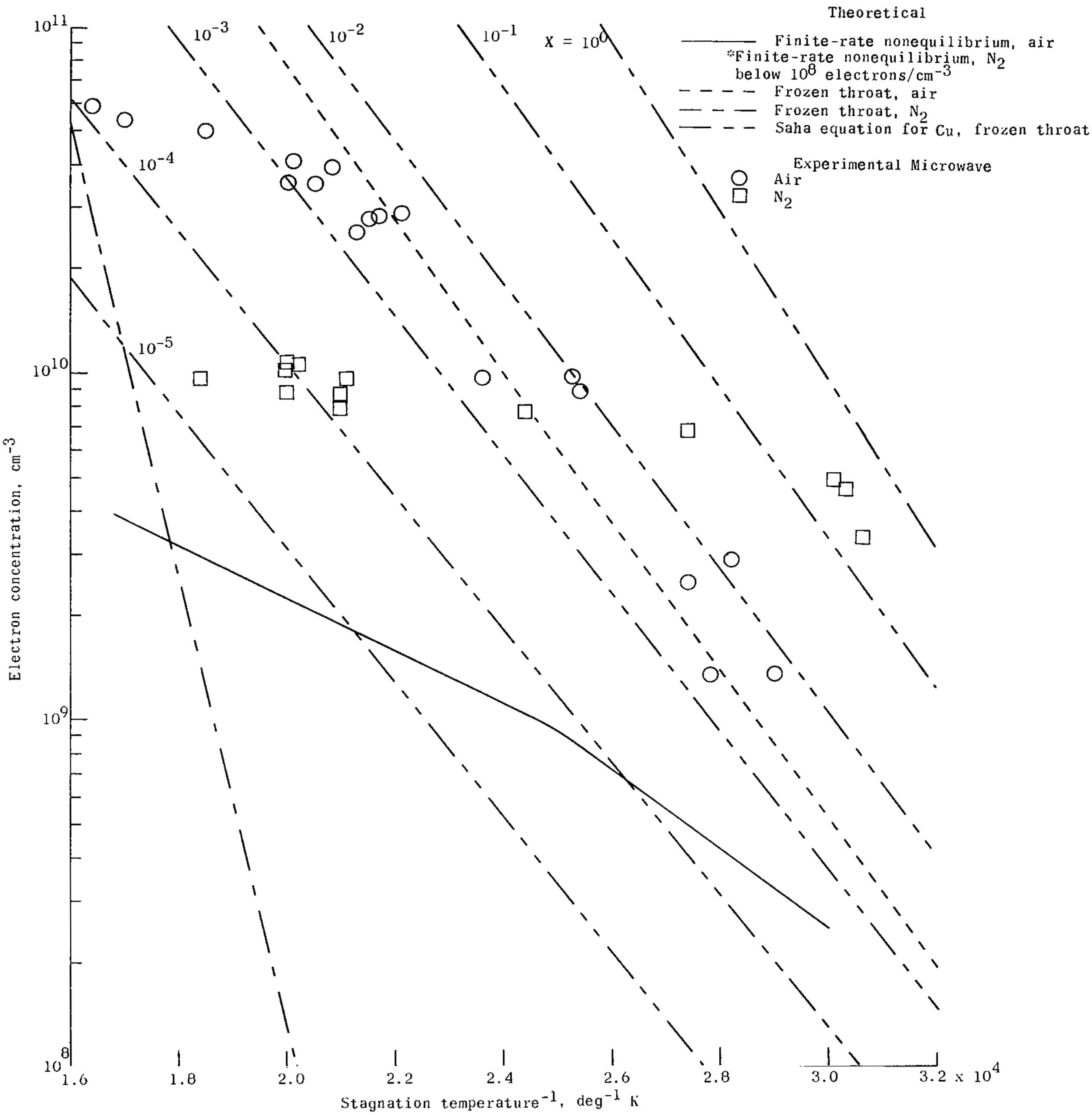

Figure 8.- Electron concentration of air and nitrogen in test section as a function of reciprocal stagnation temperature.

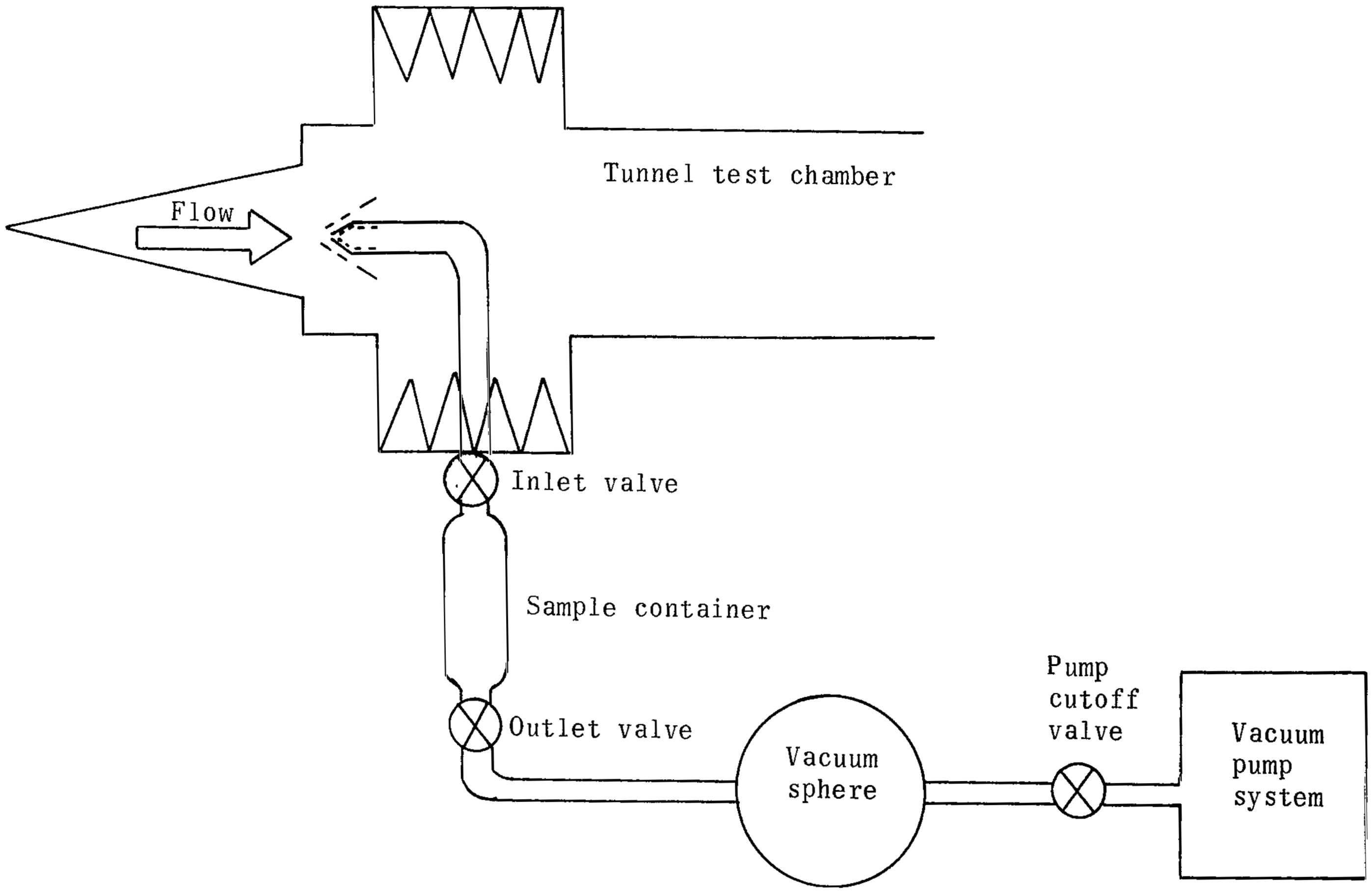

Figure 9.- Mass spectrometer sampling apparatus.

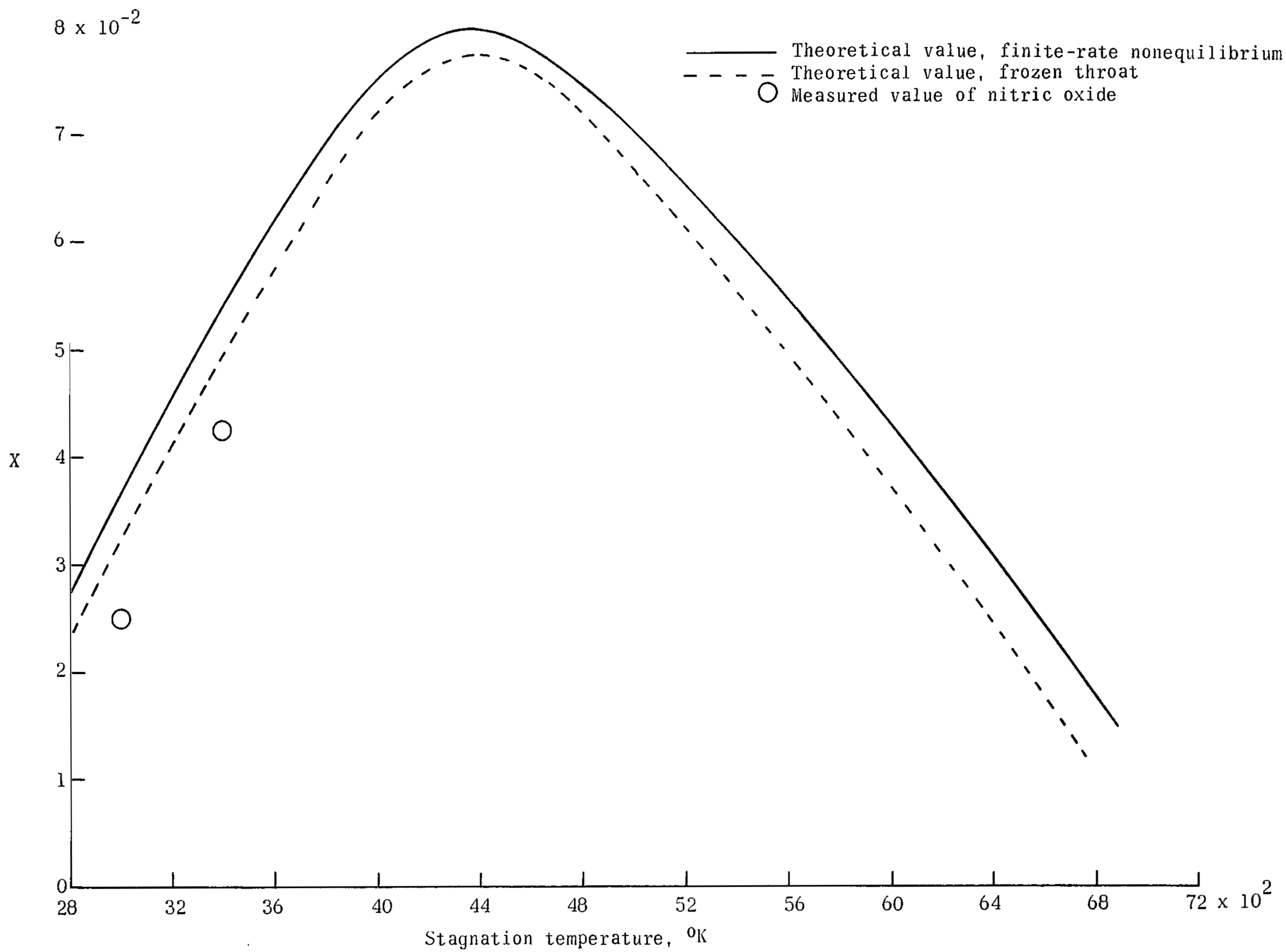

Figure 10.- Nitric oxide concentration as a function of stagnation temperature.

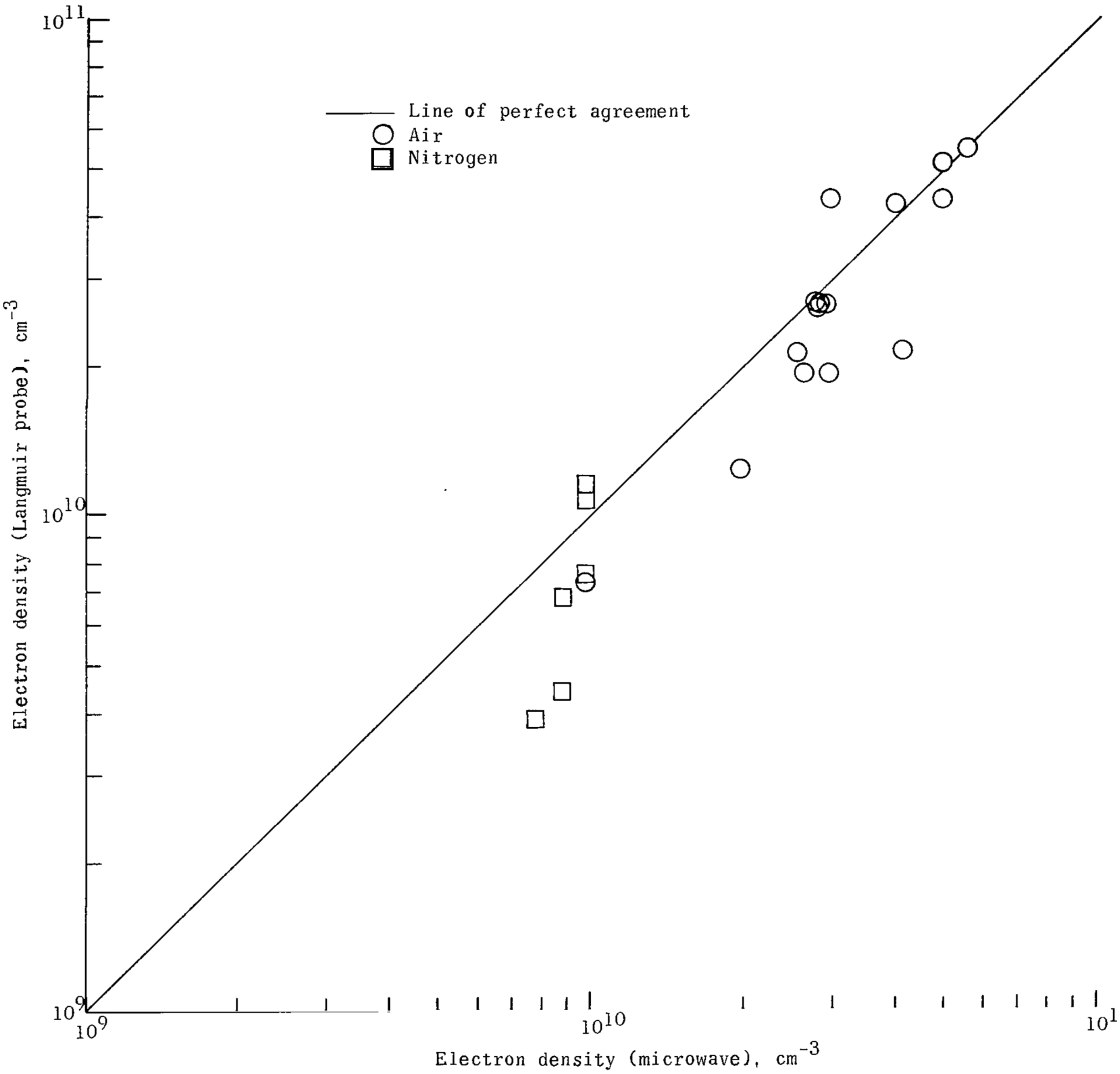

Figure 11.- Comparison of electron concentration determined by microwave interferometer and conical Langmuir probe. Ion, copper.

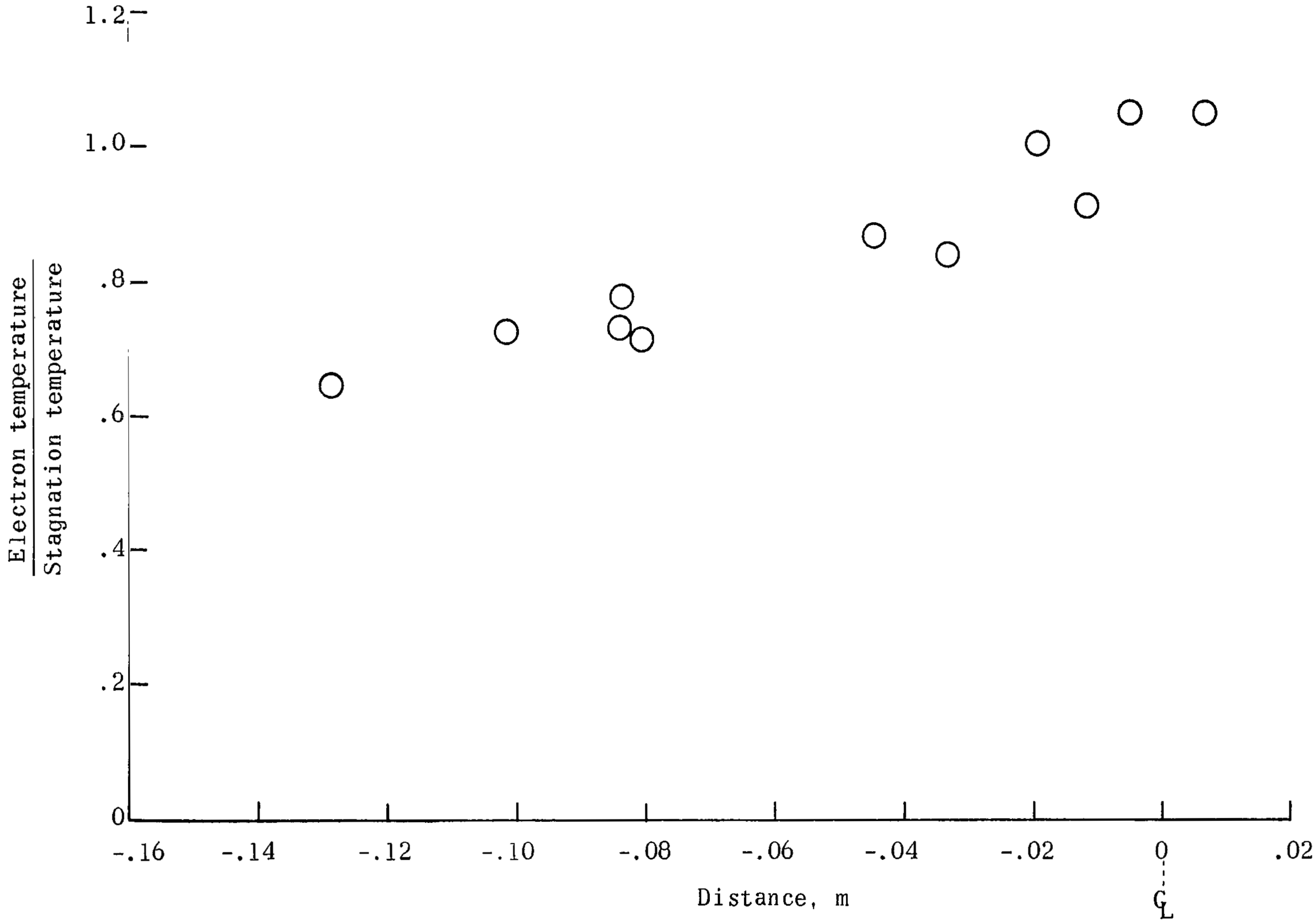

(a) Air.

Figure 12.- Electron temperature survey of the test section obtained by using a cylindrical probe.

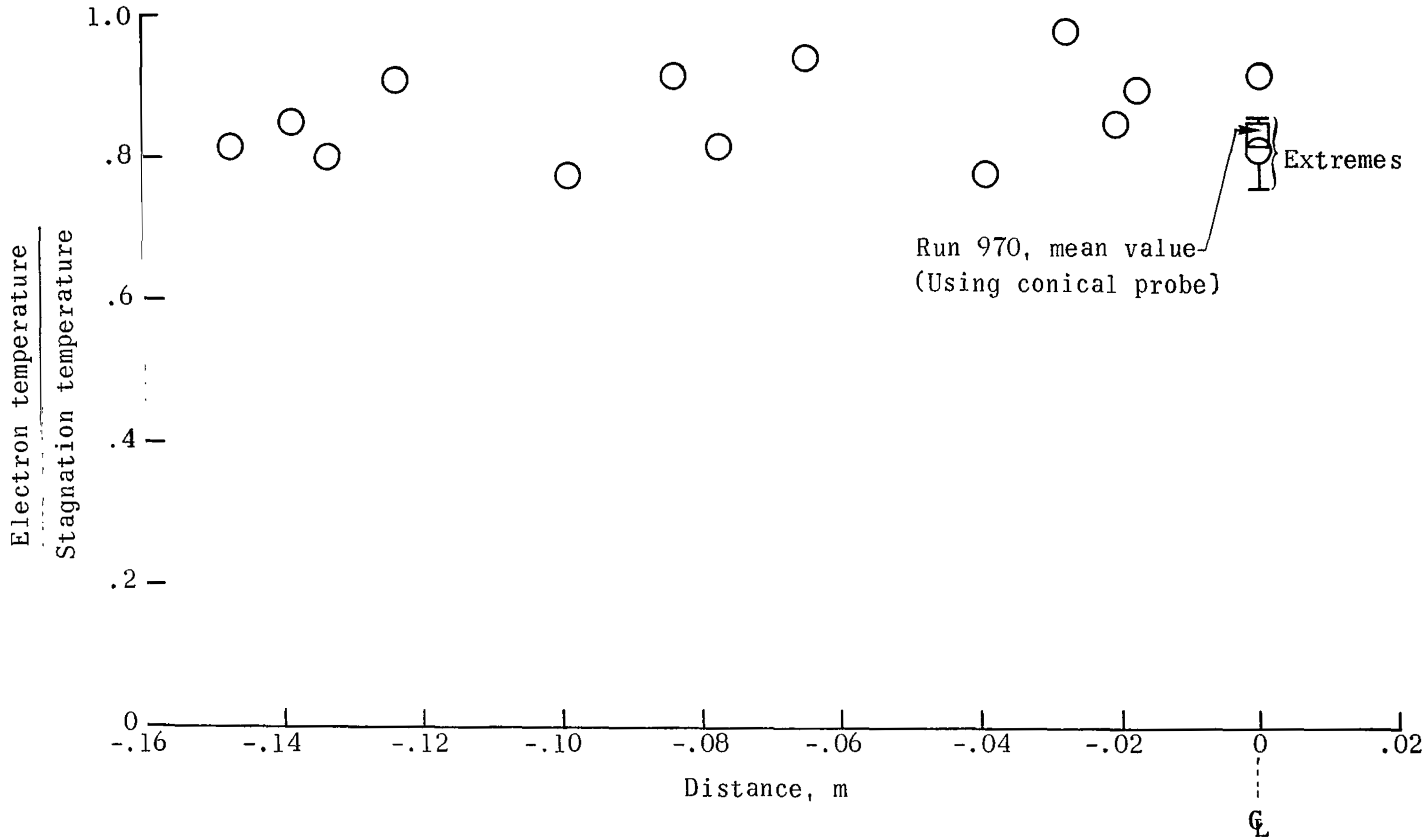

(b) Nitrogen.

Figure 12.- Concluded.

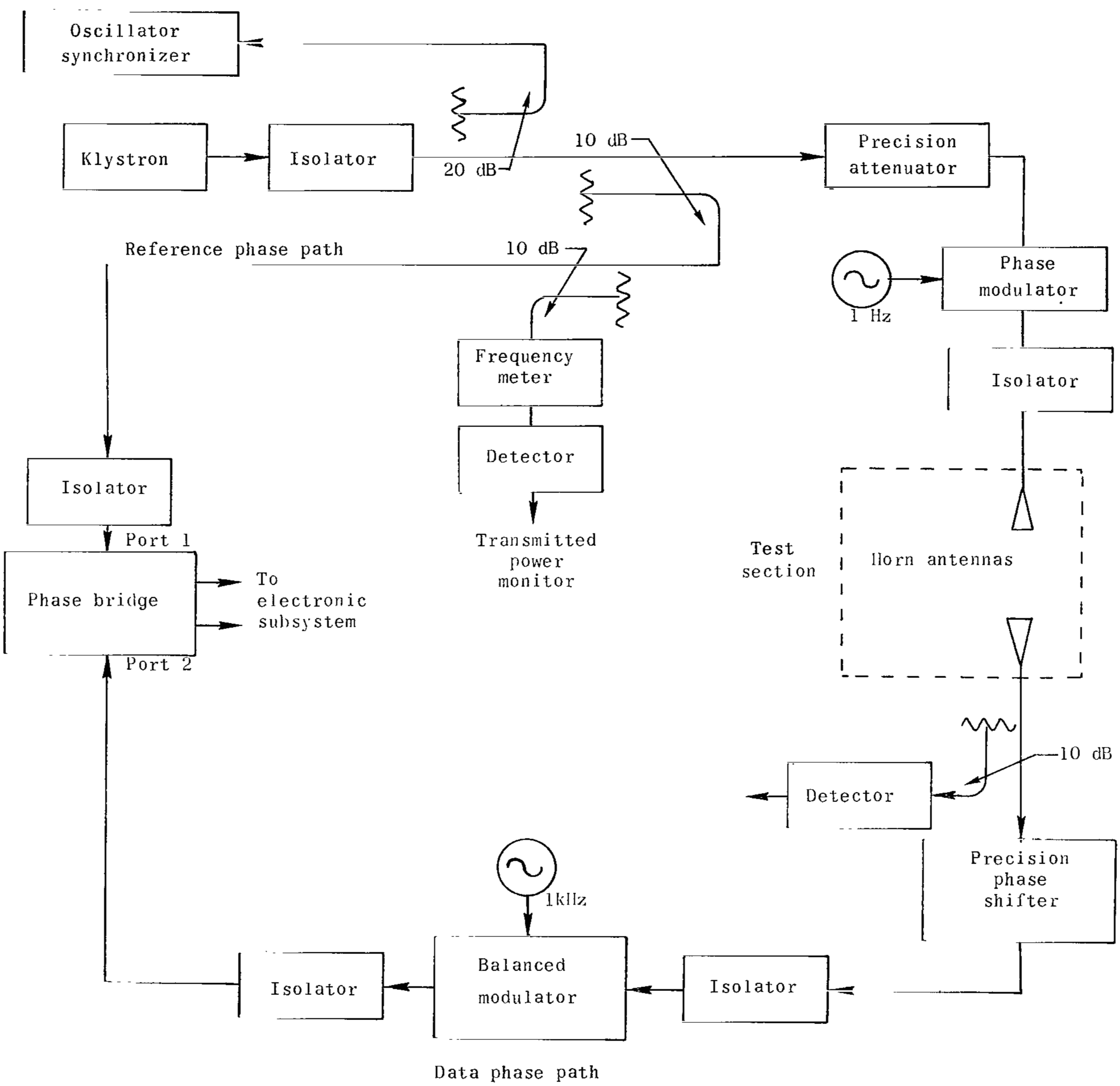

Figure 13.- The 24-GHz interferometer microwave subsystem.

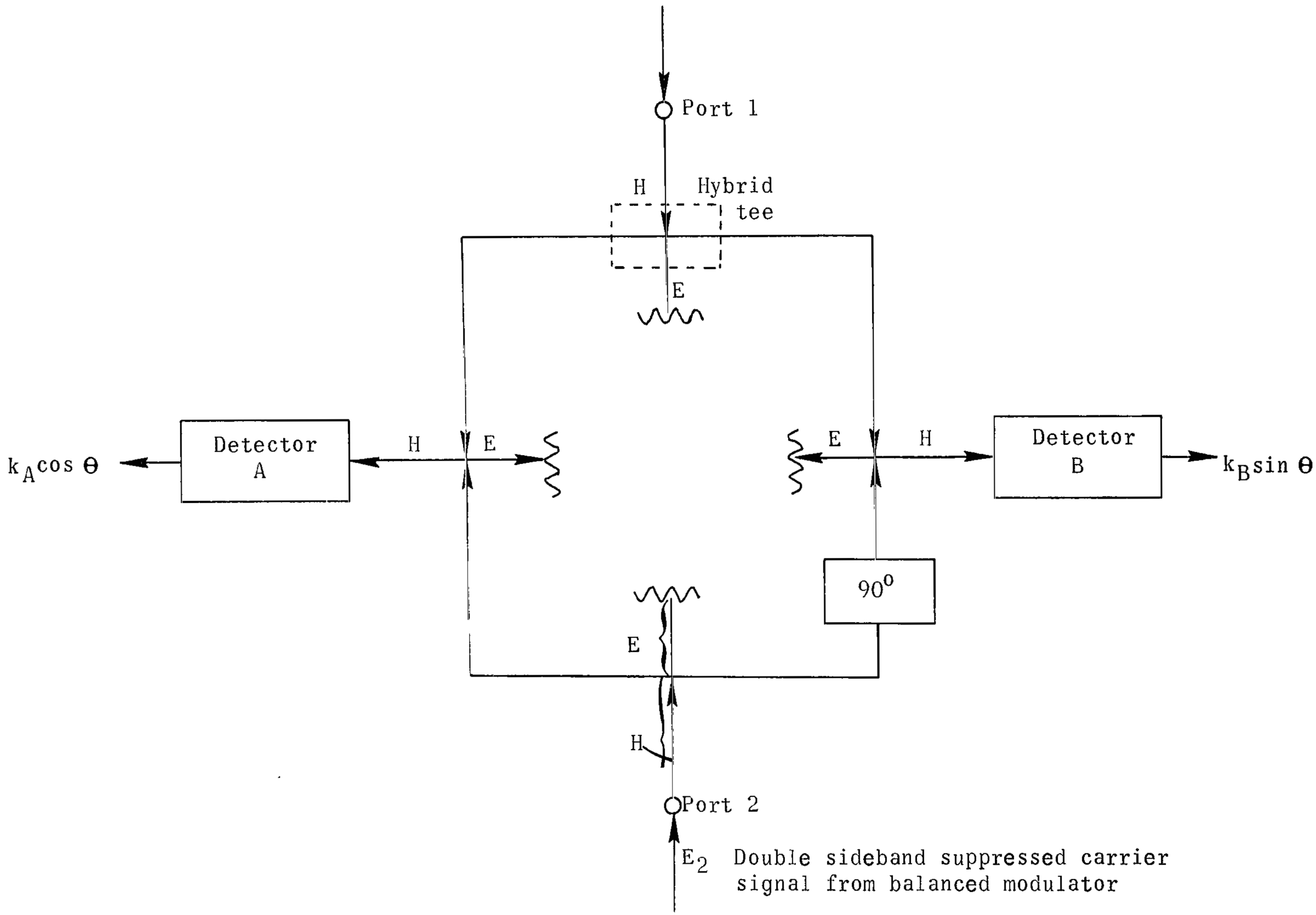

Figure 14.- Microwave phase bridge.

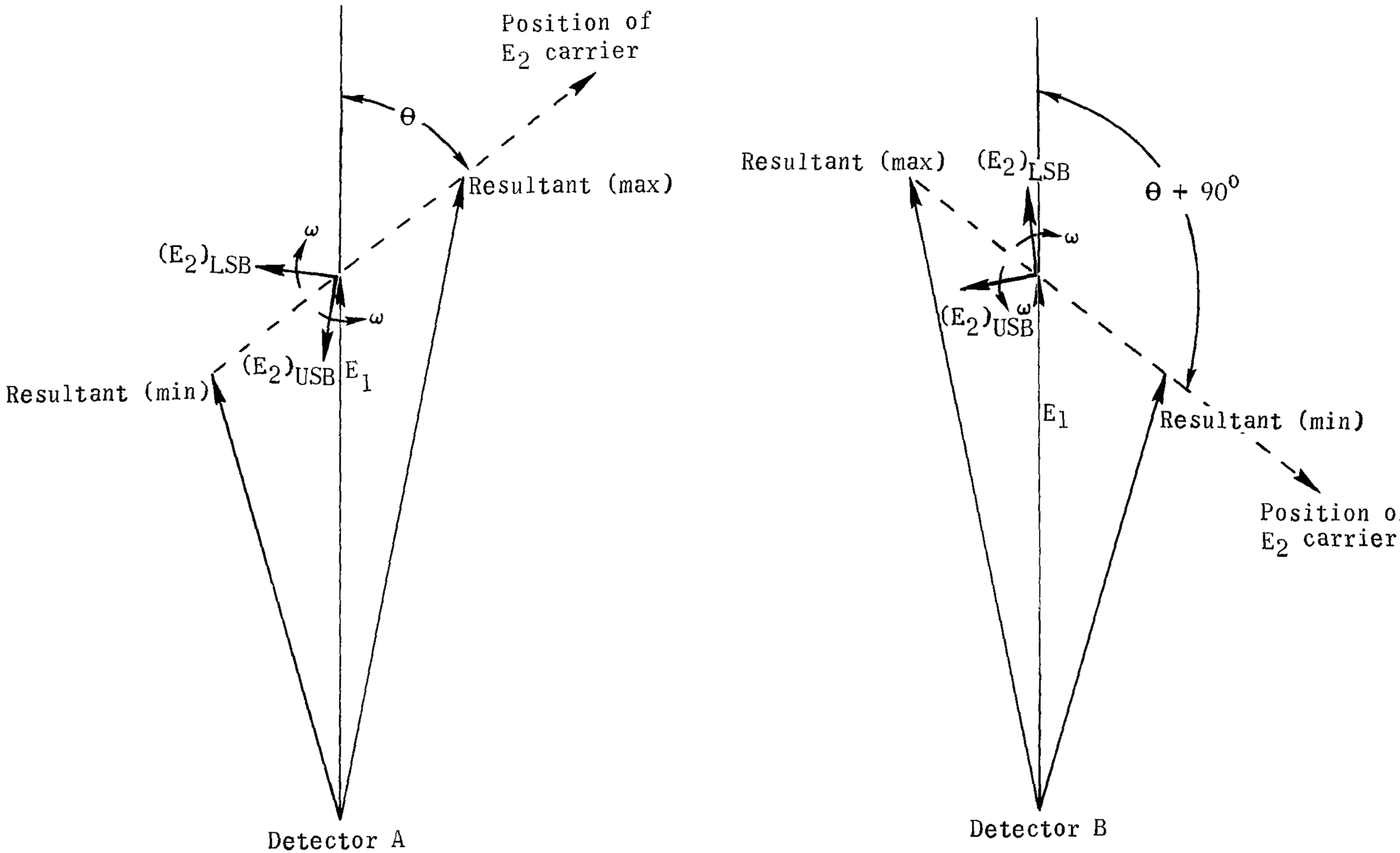

Figure 15.- Phasor addition at detectors. LSB denotes lower side band; USB, upper side band.

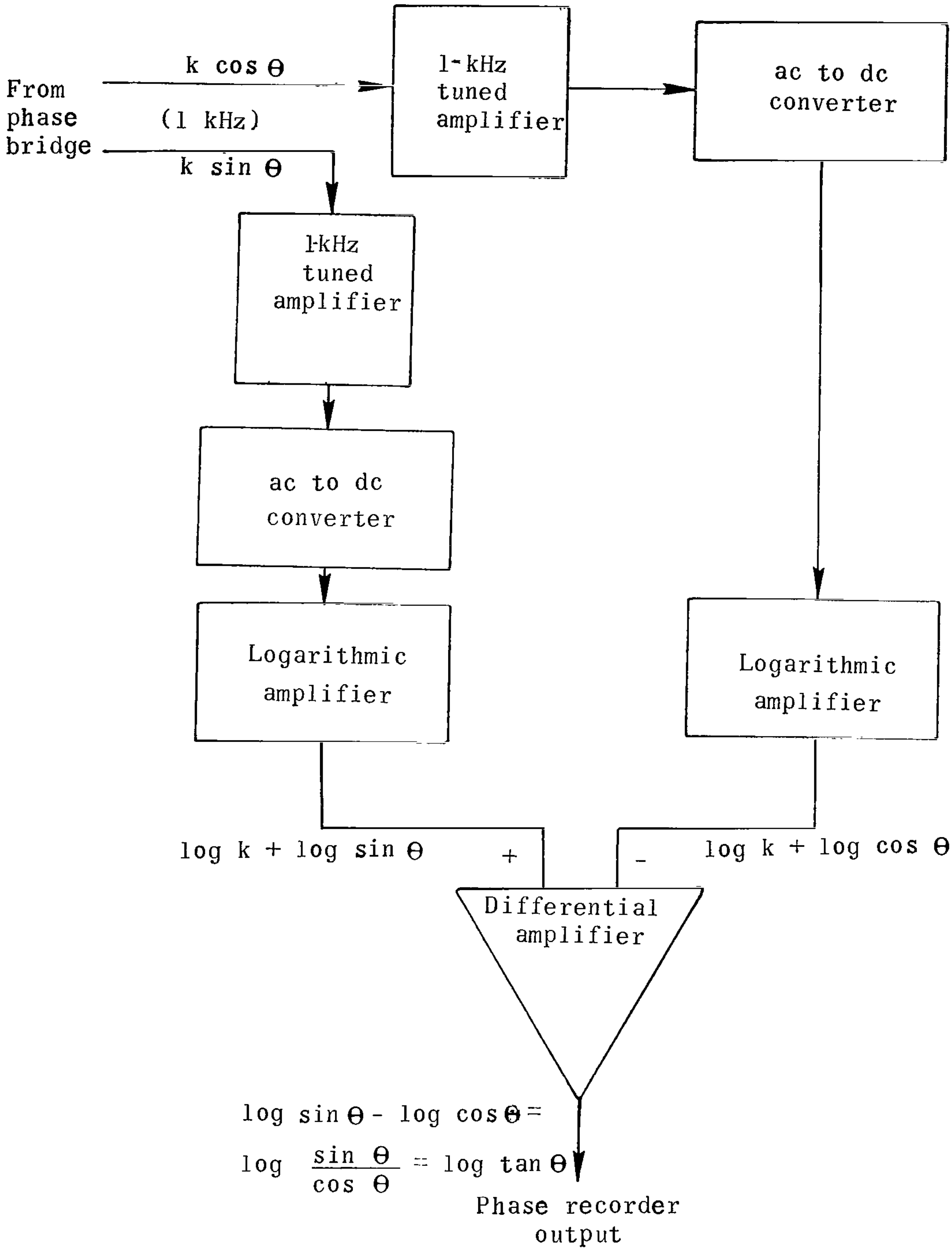

Figure 16.- The 24-GHZ interferometer electronic subsystem.

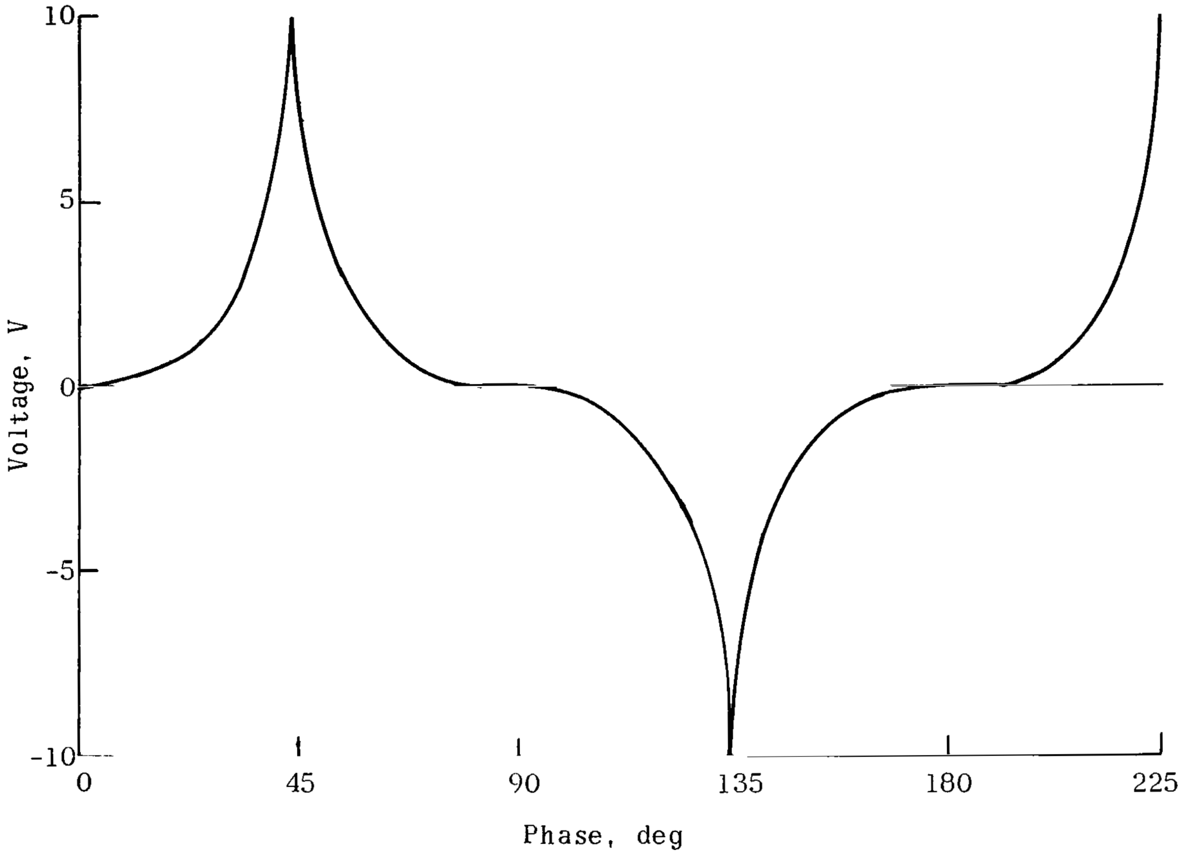

Figure 17.- Variation of output of differential amplifier with phase.

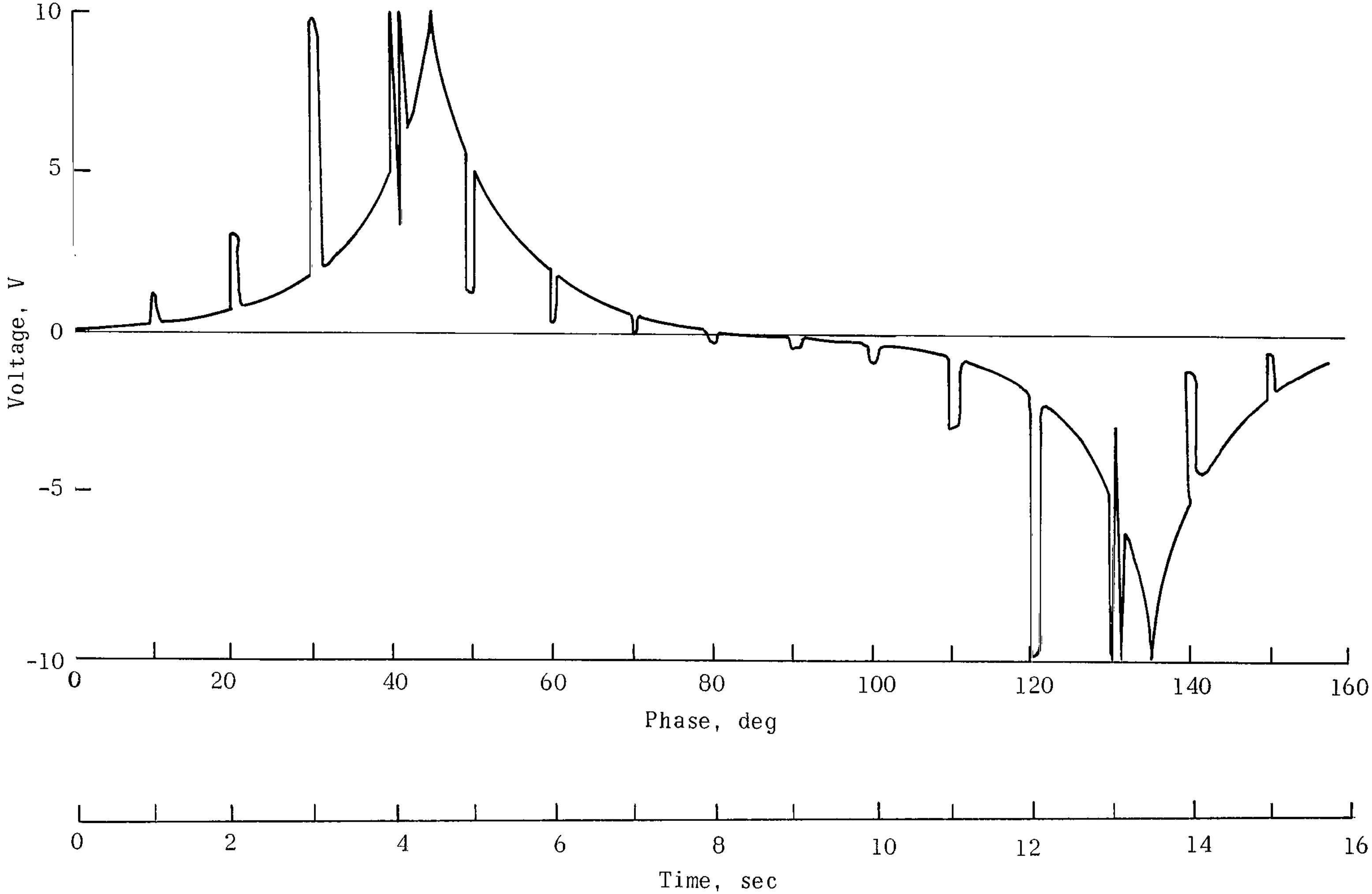

Figure 18.- Variation of output of differential amplifier with time and phase. Phase linearly increasing at 10°/sec; 15° phase pulses at 1-Hz rate.

NASA-Langley, 1969 — 25 L-6679

NATIONAL AERONAUTICS AND SPACE ADMINISTRATION
WASHINGTON, D. C. 20546

OFFICIAL BUSINESS

FIRST CLASS MAIL

POSTAGE AND FEES PAID
NATIONAL AERONAUTICS AN
SPACE ADMINISTRATION

06U 001 50 51 3DS 69286 00903
AIR FORCE WEAPONS LABORATORY/WLIL/
KIRTLAND AIR FORCE BASE, NEW MEXICO 87117

ATT E. LOU BOWMAN, CHIEF,TECH. LIBRARY

POSTMASTER: If Undeliverable (Section 158 Postal Manual) Do Not Return

"The aeronautical and space activities of the United States shall be conducted so as to contribute . . . to the expansion of human knowledge of phenomena in the atmosphere and space. The Administration shall provide for the widest practicable and appropriate dissemination of information concerning its activities and the results thereof."

— NATIONAL AERONAUTICS AND SPACE ACT OF 1958

NASA SCIENTIFIC AND TECHNICAL PUBLICATIONS

TECHNICAL REPORTS: Scientific and technical information considered important, complete, and a lasting contribution to existing knowledge.

TECHNICAL NOTES: Information less broad in scope but nevertheless of importance as a contribution to existing knowledge.

TECHNICAL MEMORANDUMS: Information receiving limited distribution because of preliminary data, security classification, or other reasons.

CONTRACTOR REPORTS: Scientific and technical information generated under a NASA contract or grant and considered an important contribution to existing knowledge.

TECHNICAL TRANSLATIONS: Information published in a foreign language considered to merit NASA distribution in English.

SPECIAL PUBLICATIONS: Information derived from or of value to NASA activities. Publications include conference proceedings, monographs, data compilations, handbooks, sourcebooks, and special bibliographies.

TECHNOLOGY UTILIZATION PUBLICATIONS: Information on technology used by NASA that may be of particular interest in commercial and other non-aerospace applications. Publications include Tech Briefs, Technology Utilization Reports and Notes, and Technology Surveys.

Details on the availability of these publications may be obtained from:

SCIENTIFIC AND TECHNICAL INFORMATION DIVISION

NATIONAL AERONAUTICS AND SPACE ADMINISTRATION

Washington, D.C. 20546